redin Revista Facultad de Ingeniería, Universidad de Antioquia, No.89, pp. 59-67, Oct-Dec 2018

Polycaprolactone- Chitosan- Ag coatings on Ti6Al4V: Critical synergic aspects analyzed by Raman, EFM and contact angle

Recubrimientos de policaprolactona- quitosano y plata sobre Ti6Al4V: Análisis de los aspectos sinérgicos críticos mediante Raman, EFM y ángulo de contacto

Sara Maria Leal-Marin[1] **Hugo Armando Estupiñán-Duran**[1*]

[1]Grupo de tribología y superficies, Facultad de minas, Universidad Nacional de Colombia. Calle 75 # 79ª-51, Bloque M17. C. P. 050034. Medellin, Colombia

ARTICLE INFO:

Received: February 12, 2018

Accepted: October 08, 2018

AVAILABLE ONLINE:

November 18, 2018

KEYWORDS:

Biocompatible coating, wettability, electric potential, polymers, bone implant.

Recubrimiento biocompatible, mojabilidad, potencial eléctrico, polímeros, implante óseo.

ABSTRACT: The Ti6Al4V presented a natural oxide layer that increased the corrosion resistance of the material but decreased the physicochemical compatibility with the bone tissue. The use of polymeric coatings on Ti6Al4V allows the creation of an interface that promotes osseointegration and antibacterial activity. The objective of this work was to analyze a coating on Ti6Al4V obtained by dip-coating with a mixture of chitosan, polycaprolactone, and silver. The synergy between chitosan and silver allows the polymeric matrix to be retained and to enhance the coating's mechanical-structural functions, integrating bone cells and serving as antibacterial agents. Coating morphology was assessed by scanning electron microscopy (SEM) and the distribution of chemical elements was determined by energy dispersive spectroscopy (EDS). Confocal Raman spectroscopy was used to evaluate the composition and structure of the coating. Electrical potential distribution, phase distribution and surface topography of surfaces were analyzed using an electrostatic force microscopy. Contact angle measurements were also performed to determine coating wettability.

RESUMEN: El Ti6Al4V presenta una capa pasiva de óxido natural que aumenta su resistencia a la corrosión, pero disminuye su compatibilidad fisicoquímica con el tejido óseo. Los recubrimientos poliméricos en la aleación de Ti6Al4V permiten la creación de una interface entre el tejido óseo y la aleación que promueva la osteointegración y otros efectos dependiendo de sus componentes, como la actividad antibacterial. El objetivo de este trabajo fue analizar un recubrimiento sobre Ti6Al4V obtenido por medio de dip-coating con una mezcla de quitosano, policaprolactona y plata. La sinergia entre el quitosano y la plata permitió retener la matriz polimérica y mejorar las funciones estructurales del recubrimiento, sirviendo como agente integrador de las células óseas y posible agente antibacteriano. La morfología del recubrimiento se evaluó por microscopia electrónica de barrido (MEB) y la composición elemental por espectroscopia de energía dispersiva de rayos X (EDS). Se empleó espectroscopia confocal Raman para evaluar la composición y estructura del recubrimiento. La distribución del potencial eléctrico, fase y topografía de las superficies se analizó usando microscopia de fuerzas electrostáticas. Y por último la mojabilidad de los recubrimientos se realizó con mediciones de ángulo de contacto.

1. Introduction

Titanium and titanium alloys are widely used in orthopedic devices and dental implants because of its corrosion resistance and biocompatibility properties [1]. However, these characteristics can be improved to obtain more compatibility between the material and the physicochemical properties of bone tissue. In order to reach this similitude level, various coating techniques had been used such as sputtering, electrophoretic deposition, ion implantation, sol-gel, plasma electrolytic oxidation, dip-coating, among others [2, 3].

Coatings obtained by the dip-coating technique allow the incorporation of polymers dissolved in an aqueous solution to the material surface. This coat protects the

* Corresponding author: Hugo Armando Estupiñan Duran
E-mail: haestupinand@unal.edu.co
ISSN 0120-6230
e-ISSN 2422-2844

DOI: 10.17533/udea.redin.n89a08

metal from corrosion when brought into contact with the physiological fluid and generates an osteogenic contact interface. The coating can act as a biodegradable and specialized scaffold. A scaffold facilitates cell growth, which can gradually be replaced by bone structures of high mechanical and biochemical functionality. For this work, polycaprolactone (PCL) was used due to its tendency to favor the production of extracellular matrix [4]. However, PCL hydrophobicity hinders uniform protein distribution and cell adhesion. To modify PCL wettability different types of solvents have been extensively used to promote the formation of a hydrophilic surface, including polymers such as chitosan, collagen, and acrylates [4, 5]. Chitosan (Q) is a natural polymer widely used in matrices for bone cell growth. Q positive charge favors the reaction with anionic functional groups responsible for regulating cellular activity [4]. Additionally, elements such as silver have been used in coatings to inhibit the growth of biofilms and bacterial growth on implanted devices. The Q and Ag ions promote activity against gram-positive and gram-negative bacteria [4, 6].

Chitosan, polycaprolactone, and Ag together present promising characteristics for applications in the regeneration of bone tissues due to the mechanical, physicochemical and degradation properties of PCL, coupled with the bioactive and antibacterial characteristics of Q and silver. Also, the presence of Q and Ag may reflect important morphological, topographical and electric charge variations, which would improve wettability and surface tension, in a fashion that would favor bone contact.

The aim of this work was to analyze the critical synergistic aspects conjugated in the properties of coatings of polycaprolactone, chitosan, and silver. Those aspects were assessed through the evaluation of the morphology, topography, wettability, composition, and surface energy to discuss the use of this type of coatings in osteosynthesis applications. Topography, composition, surface energy and wettability of the implant surface conditioned the action of proteins, ions, lipids, sugars, and molecules present in the blood; regulating the interaction of the material with physiological processes, mainly of cell adhesion, [7, 8].

2. Materials and methods

2.1 Sample preparation

Ti6Al4V ELI disks of 14 mm diameter and 3 mm thickness were employed. These disks were polished with SiC. After grinding, they were immersed in an ultrasonic container for 5 min in isopropyl alcohol, rinsed with distilled water and dried at room temperature. Before the alkaline treatment, a process of pickling of unstable oxides was carried out on the Ti6Al4V disks with 3% HF and 20% HNO_3 keeping the disks immersed for 20 s. Then, disks were rinsed with distilled water, isopropyl alcohol and stored in a desiccator until the dip-coating and the characterization tests were carried out.

2.2 Alkaline treatment

The alkaline treatment promotes the adhesion of hydroxyl groups on the Ti6Al4V surface through the formation of a layer of sodium titanate. Alkaline treatment has been shown to be efficient to generate preferential sites for hydroxyapatite deposition [9]. Ti6Al4V samples previously polished and pickled were immersed in a 10 M NaOH solution for 24 h at 60°C to promote titanate formation. Afterward, samples were rinsed with distilled water and dried in an oven at 100°C for 24 h. Later, samples with alkaline treatment were subjected to a heat treatment to stabilize the sodium titanate layer. The heat treatment was performed in a muffle at 450°C for 1 h with a heating ramp of 10°C/min and cooled down to room temperature inside the muffle.

2.3 Dip-coating and silver sputtering

Dip-coating was employed to obtain polymeric coatings on Ti6Al4V. For polymeric coatings, three different solutions varying Q concentration (0.1, 0.2 and 0.3 g/L of Q) and one PCL concentration (0.3 g/L) were used. Q concentrations were dissolved in 0.5 M acetic acid at room temperature until complete dissolution. PCL was dissolved in 99% glacial acetic acid with permanent stirring at 1000 rpm for 2 h. Solutions of Q and PCL were mixed in a (v/v %) ratio of 30%-70% until a homogeneous solution was obtained.

For dip-coating, Ti6Al4V disks were immersed in the 3 solutions described with a speed of 4.1 cm/min and kept immersed for 10 s. Three immersions were performed to obtain 3 polymeric layers. Between the second and the third immersion, a sputtering treatment was performed to deposit a thin film of silver. Between each dipping, samples were heated in an electric oven at 55°C for 30 min to promote solvent evaporation.

For the sputtering process, samples were placed in a sputtering (Q150R, Quorum) using a silver target of 1 mm thickness and two deposition times, 120 s and 240 s, with a current of 50 mA. The thickness of the silver coat was measured with an internal quartz sensor in the equipment. The samples were subsequently kept in an oven at 100°C for 1 h to fix the powdered silver with the polymer matrix.

Finally, the last immersion was performed to obtain a third layer of polymeric coat. Samples were heated at 50°C for 1 h and stored in a desiccator for posterior

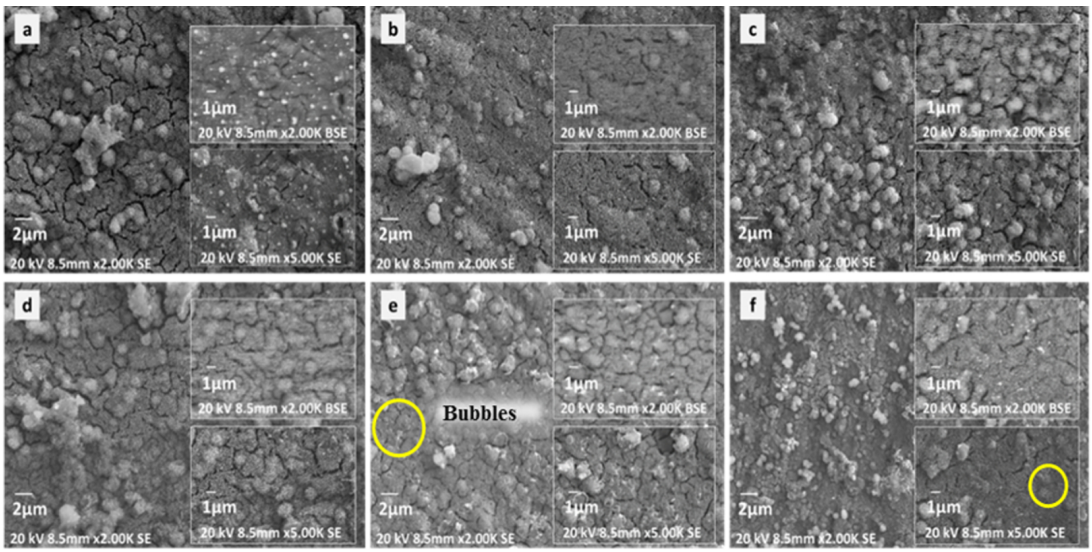

Figure 1 Coatings obtained by dip-coating at different concentration and time deposition of Ag **a)** 0.1Q-PCL 120s Ag, **b)** 0.1Q-PCL 240s Ag, **c)** 0.2Q-PCL 120s Ag, **d)** 0.2 Q-PCL 240s Ag, **e)** 0.3Q-PCL 120s Ag and **f)** 0.3Q-PCL 240s Ag. (Bubble formation marked with circles)

characterization. Sample identification was established naming Q concentration and time of silver deposition, i.e. 0.1Q-PCL 120s Ag.

2.4 Morphological and compositional characterization

Scanning electron microscopy (SEM) and energy dispersive X-Ray spectroscopy (EDS)

Morphological identification of the samples was performed with a SEM equipment (EVO MA10, Carl Zeiss) and an elemental compositional analysis was assessed by EDS with an X-Act detector (Oxford Instruments) employing INCA software as an acquisition tool. An acceleration voltage of 20 kV was used.

X-Ray Diffraction (XRD)

A powder diffractometer (D8 ADVANCE, Bruker) with CuKαl radiation, the acceleration voltage of 40 kV, a divergence grid of 0.6 mm, a measuring range of 10° to 65° in 2θ, a stepwise sampling of 0.01526° and a sampling time of 1 s were employed. The qualitative analysis of the phases was done by comparing the profile given in the database PDF-2 Center for Diffraction Data (ICCD).

Confocal Raman spectroscopy

Spectral composition analysis was performed using a confocal Raman spectrometer (LabRam HR, HORIBA) with a 532 nm laser at a power of 15 mW. The spectra were taken in a range of 0 to 1500 cm^{-1} with an acquisition time of 3 s.

Electrostatic force microscopy (EFM)

Electrostatic force microscopy was acquired using an atomic force microscope (NX10, Park Systems). EFM assesses the electrical potential, phase and sample amplitude in scanning mode kelvin probe mode (EFM-SKPM). A conductive tip of Cr/Pt-coated (Multi 75E, Budget sensors) with a force constant of 3 N/m and a resonance frequency of 75 kHz was employed. Mappings of 10x10 μm were performed with a scan rate of 0.4 Hz. For EFM after obtaining the image of height (topography), the tip performed a second scan with a potential in the sample of -2 V and an amplitude of 1.5 V. From the height images, the roughness factor Rq was reported. This parameter is defined by the square root of the mean of the squares of the height deviations taken in relation to the mean data of the measurements.

Contact angle measurements

The wettability measurements were performed on a commercial contact angle device (Model 200, Ramé-hart). The contact angle was measured using the sessile drop method and distilled water as the polar substance. 20 measurements per sample were taken every 0.5 s. Using the DROPimage Standard software, the average contact angles for each sample and the surface energy were calculated.

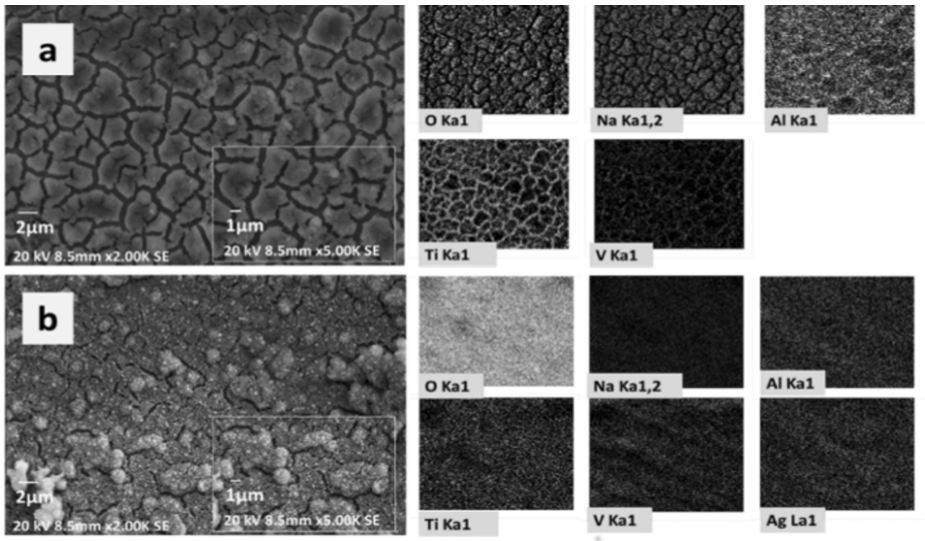

Figure 2 EDS mapping of the coated samples. **a)** Ti6Al4V after the alkaline treatment and **b)** 0.1Q-PCL 120s Ag

3. Results and discussion

3.1 Morphological and compositional characterization

SEM

Coatings obtained with different PCL-Q-Ag concentrations (Figure 1(a-f)) presented heterogeneous morphologies with the formation of porous agglomerates in flower shape. This shape is characteristic of Q presence. In addition, porous agglomerates are characteristic of PCL films obtained with acetic acid as solvent [5]. It was noticeable that an increase in Q concentration also increased the agglomerations as Figure 1(a and e) presented. Also, the agglomerate size decreases as the Q concentration increase. Samples coated with 0.1Q-PCL presented a coat of less thickness and less structure, this could be noticed in the grain morphology. Grain morphology is like the one observed in samples of Ti6Al4V after the alkaline treatment (sodium titanate (Figure 2(a))) without polymeric coating. This grain morphology was not distinguishable in samples with a higher concentration of Q, because low uniformity of the coating was related to Q concentration.

Backscattered electron (BSE) images of Figure 1 (presented in detail in the first box on the right side from top to bottom for each figure (a), (b), (c), (d), (e), (f)) show the silver particles that were included in the coating after sputter deposition. A significant difference in morphology was not observed between the two deposition times. This was because the thicknesses variation of the silver film with 120 s and 240 s of time deposition was not significant. Moreover, Figure 1(e and f) corresponding to 0.3 g/L of Q presented bubble formation in the coating (marked with circles). These bubbles may be caused by trapped gas between the sodium titanate and the polymer coating when acetic acid and water used as the solvent were evaporated. This phenomenon has been previously reported for this type of coatings especially when the volume-volume relationship between Q and PCL presented a variation [9].

Morphological analysis and topographic analysis given by atomic force microscopy may reveal the biocompatibility of the polymeric coating. It may also illustrate the relationship between bone tissue and an implantable device coated for fracture healing processes. Some researchers have shown that differences in surface topography, including texture and roughness of implantable devices, have affected the adsorption of fibronectin and albumin according to reports in vitro studies and cell adhesion [7, 10]. Osteoblasts have been shown to be sensitive to surface microarchitecture, and osteosarcoma cells have presented reductions in cell growth and differentiation related to topographical changes in the surface [7, 11].

EDS

EDS analysis carried out on the surfaces presented the main elemental chemical components of the coatings obtained as shown in Figure 2. Figure 2(a) shows the Ti6Al4V sample after the alkaline treatment. Alkaline treatment has improved sodium titanate formation on samples surface. This titanate formation may be related to the uniform distribution of oxygen, sodium, and titanium in granular shapes. A Higher presence of titanium, aluminum, and vanadium was also detected at the crack sites between the grains which are characteristic of the

Table 1 EDS sample composition for different coatings

%Atomic	O K	Na K	Al K	Ti K	V K	Ag L
Alkaline treatment	64.19	9.07	1.20	24.82	0.73	–
0.1 Q-PCL 120s Ag	57.79	2.65	1.65	32.81	1.05	1.96
0.1 Q-PCL 240s Ag	54.53	4.8	1.29	31.42	0.93	1.59
0.2 Q-PCL 120s Ag	60.73	6.24	1.24	29.26	0.98	1.57
0.2 Q-PCL 240 s Ag	60.89	4.80	1.56	30.31	0.81	1.63
0.3 Q-PCL 120s Ag	57.73	5.57	1.72	32.07	1.01	1.67
0.3 Q-PCL 240s Ag	58.99	5.66	1.63	31.03	1.04	1.66

Ti6Al4V composition without any coating.

Maps showed in Figure 2(b) for samples 0.1Q-PCL 120s Ag confirmed the uniformity of the polymeric coat. The fact that the grain morphology presented in the uncoated samples (Figure 2(a)) did not appear in this case (Figure 2(b)) provided further evidence to support the uniformity.

The elemental composition presented in Figure 2 was summarized by semi-quantitative results shown in Table 1.

According to the semi-quantitative results presented in Table 1, samples did not present significant variations in their elemental composition. Only a notable decrease in sodium was observed in relation to the sample just with alkaline treatment and this sodium percentage varied from approximately 9.07% to 4.95% in atomic composition. This phenomenon may be for an elimination of sodium from the titanate compound during the polymeric coating process. It is also observed that the composition of deposited silver was in the range of 1.57% to 1.96% independently of the deposition time used. This small difference in composition was possibly due to the thickness of the silver coating obtained. It was for a 120 s deposition of 9.4 nm, differing only in 0.9 nm with the 240 s deposition which was 10.3 nm.

XRD

XRD presented in Figure 3 corresponds to the result of the sample of Ti6Al4V with alkaline treatment, confirming the presence of sodium titanate which had previously been mentioned. Moreover, it showed the presence of metallic titanium from the substrate, and oxides of titanium generated by the thermal treatment in the surface. The peaks at 27, 38, 48, 54 and 58° correspond to the crystalline phase of TiO_2 in the form of anatase. Other research after the alkaline treatment presented a crystalline phase of TiO_2 in form of rutile [12, 13]. This phase was influenced by higher temperatures in the alkaline treatment and posterior heat treatments around 600°C for the Ti6Al4V samples [13]. This phase is desirable for stability and enhances the anticorrosive properties. However, the samples analyzed did not have strong bulk presence of this phase (the superficial Raman spectroscopy Figure 4, showed some peaks related to rutile) possibly for the short time of heat treatment employed.

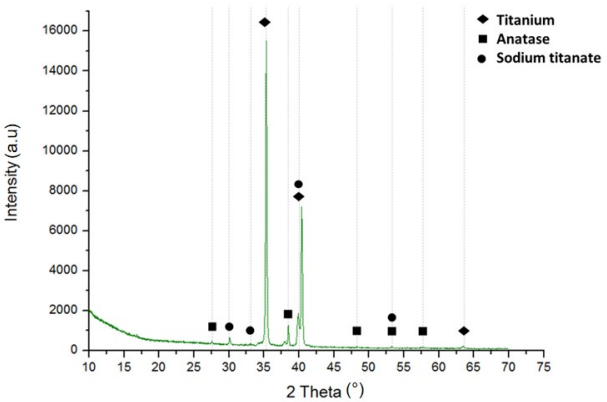

Figure 3 XRD spectrum for the sample of Ti6Al4V after the alkaline treatment

The peaks at 35, 40 and 54° correspond to the metallic titanium present in the Ti6Al4V substrate [2, 14] and the peaks at 30, 33, 40, 53° are characteristic of the sodium titanate in Na2TiO3 form. Other researchers have reported these same peaks for $Na_2Ti_5O_{11}$ [12, 13]. Sodium titanate has been considered an intermediate between polymeric coatings and metal substrates since in its hydrated state it has a gel configuration that allows the chemical-physical union of the polymer with the substrate. In the case of the configuration proposed in this research, this compound can efficiently unite the polymer chains of polycaprolactone and chitosan. The $HTiO_3^-$ group attracts the Na^+ cations, to form a sodium titanate gel on the surface during dehydration, consolidating a stable and amorphous solid. Upon contact with a fluid, the layer is hydrolyzed and the sodium cations are released again, leaving the $HTiO_3^-$ free, as a nucleation point of the polymeric layers of chitosan and polycaprolactone [15].

Confocal Raman spectroscopy

Spectra obtained by Raman presented in Figure 4 confirmed in the presence of titanium oxide in anatase and

rutile phase in samples. As well as the metallic titanium and sodium titanate that had been evidenced in the XRD spectrum. These phases were observed in the spectra of all samples analyzed. Sodium titanate, depending on its stoichiometry, showed wide peaks at 285cm^{-1} and at 740 cm^{-1} [16]. Rutile had peaks at 220, 450, 610, and 800 cm^{-1} and anatase at 142 and 200 cm^{-1} [17, 18]. The Raman technique has been used to differentiate the amorphous phases of crystalline formed in processes of oxidation of metals, specifically in titanium and its alloys. The presence of titanium oxide phases in the form of brookite and rutile are important owing to the fact that they have been proven very specific functions in the bioactivity of biomaterials for dental and bone use in general. The works referring to Raman characterization show the presence of brookite between 162 and 171 cm^{-1} in processes of aqueous transformation and peaks between 400 and 600 cm^{-1} referring to crystalline phases of rutile [18], which agrees with the results obtained in the Raman characterization of this work. This phase configuration demonstrates the good integration of the coating components shown in the morphological analyzes of Figure 1.

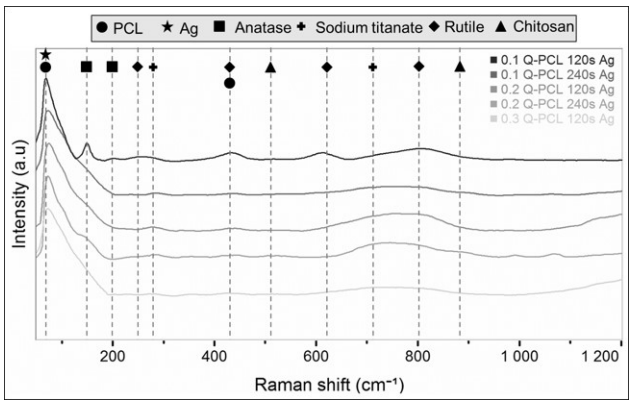

Figure 4 Raman spectra of the treated samples

In addition, this technique confirmed the presence of Q and PCL in the samples obtained. PCL showed a characteristic peak at 84 cm^{-1} and at 420 cm^{-1}, which were identified in all the samples treated. A characteristic peak at 84 cm^{-1} was related to the silver present in the coating because it coincided with the silver oxide peak. The peak of this oxide has been previously reported by other researchers with this same value [19]. Q was observed with a peak at 530 cm^{-1} and at 894 cm^{-1} which were only evidenced in samples with 0.3 g/L of Q, the one with the highest concentration.

EFM

EDS results showed that the amount of Ag contained in the coatings was similar for the samples at 120 s and 240 s of deposition times. EFM results were considered only for the samples with different concentrations of Q at 120 s of Ag deposition since in parallel their similarity was verified with those obtained at 240 s. Figure 5 shows the results of topography (height), amplitude, phase and potential for the different coatings. Height images presented agglomerates in the coating with an average width of 2 µm and an average height of 200 nm. Amplitude images presented a similar distribution in the different samples. This similarity reflects the topography obtained. Regarding the phase images, no large differences were observed between the samples. The distribution of phases in the coatings is due to the presence of the two polymers Q-PCL, as well as to the presence of Ag.

PCL is known to possess a neutral electrostatic charge and it may be identified as a constant phase in the image. When a change in the phase occurred, these may have been related to the presence of Q and Ag. Q and Ag are constituents with an electrostatic charge of cationic character. Other investigators have shown that variations in the oscillation of the tip of the cantilever in the surface scan are the reflection of a phase change that is related to the electrostatic charge of the polymers used [4].

The value of Rq was obtained using XEI software from Park Systems, according to the images obtained with the AFM. For the sample of 0.1Q-PCL 120s Ag, an Rq of 242.33 nm was obtained and a value of 144.16 nm and 148.91 nm were determined for 0.2Q-PCL 120Ag and 0.3Q-PCL 120Ag, respectively. With the increase in the concentration of Q agglomerates of a smaller size were obtained in the coating. This size was directly related. to the roughness value obtained. An average for the three types of the coating of Rq was 178.47 nm which was a value close to the value of Rq of 150 nm reported in PCL matrices dissolved in acetic acid [5]. Similarly, it has been reported that the roughness increases with a higher concentration of PCL. In this work with a Q-PCL ratio (v/v) of 30%-70%, it was expected that this type of coating presented greater roughness than those having a PCL composition of less than 70% [4]. These characteristics of roughness are very important since it has been reported that a greater roughness improves the bone-implant contact or in this case bone-coating [7]. In the case of fibroblasts cultured on Ti6Al4V, it has been reported that the cell proliferation is greater, as long as the roughness is less than 1 µm [8], so it is expected that with the roughness values obtained in the present investigation, a correct cell proliferation can be present.

In the EFM-SKPM, potential images of the obtained samples, clearer areas (greater potential) were observed with an electrical potential of approximately 100 mV. These zones were attributed to silver as differences in chemical contrast observed in the BSD images (Figure

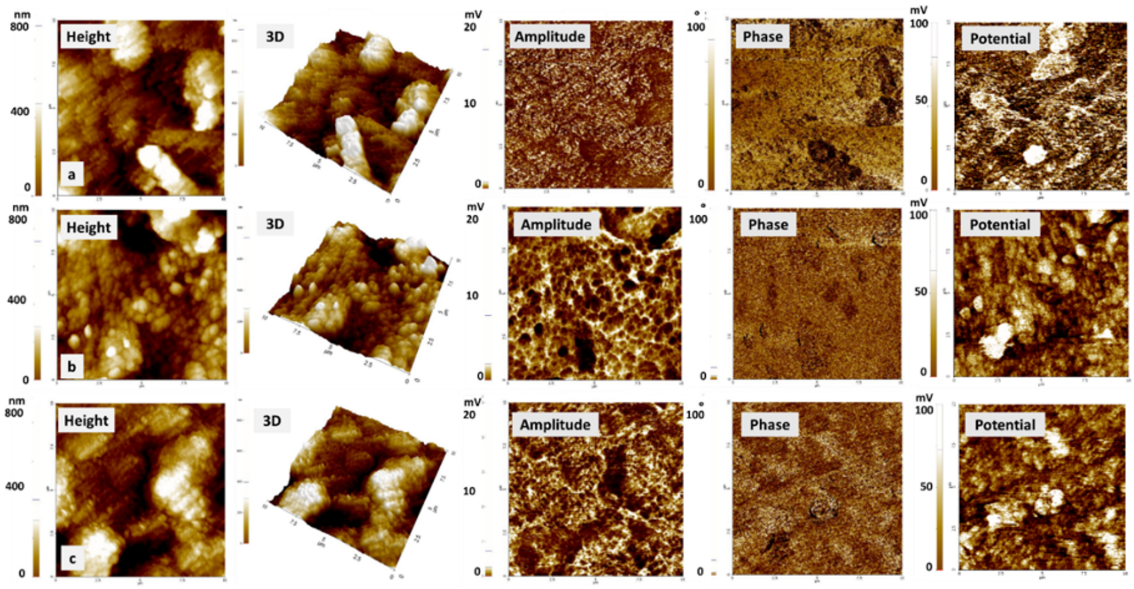

Figure 5 EFM images. Height, amplitude, phase and surface potential for the samples. **a)** 0.1Q-PCL 120s Ag, **b)** 0.2Q-PCL 120s Ag, **c)** 0.3Q-PCL 120s Ag

1) were shown. In addition, its metallic nature can be verified because the electrical potential of these areas is approximately 30 mV, which is greater than the potential of the other areas of the coating. With a potential difference of almost 3 times between the zones that are related to the presence of polymers and silver. These variations in potential may be useful in conductive properties applicable to osteosynthesis processes.

Analyzing the electrical potential, an approximation of the conductivity of the coating was presented when it was stimulated by a constant voltage. The analysis of the electrostatic potential is an observation that made in air atmosphere allowed dopants identification in materials. In this work, it allowed the identification of the silver particles included in the coating [20]. This test may be supplemented by future electrical or electrochemical impedance spectroscopy analyses to determine the behavior of the samples in contact with a simulated body solution similar to the work made by Estupiñán et al. [21]. Furthermore, biomineralization test to assess the capacity for the deposition of hydroxyapatite on the surface after a prolonged immersion time should be performed. This hydroxyapatite deposition would allow the analysis of the capacity of extracellular matrix formation in this type of coatings and its degradation process with quantitative values related to the load variations of the surface and the interfaces involved.

Contact angle measurements

The contact angle is one of the surface factors that indicate its relation to the compatibility with a biological system. Depending on the wettability, adhesion of proteins and other macromolecules to the surface will occur, like the interaction with cells, the formation of bone tissue, bacterial adhesion, the formation of biofilms and osseointegration rate [22, 23]. Figure 6 shows the contact angles obtained in the different samples analyzed.

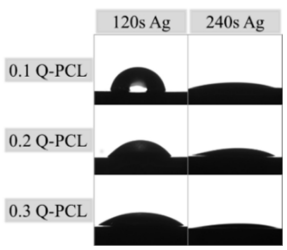

Figure 6 Contact angle images for different samples

In general, from the data presented in Table 2, it is possible to observe that for lower concentrations of Q the contact angle was higher. However, these concentrations related to higher Ag deposition time presented smaller contact angles, even though the EDS did not find significant differences in Ag content. This phenomenon occurs because longer deposition times means more surface energy applied by the sputtering on the surface. With increased energy, the silver particles will have the ability to form an oriented and polarized structure more orderly that will increase the wettability. This effect has been reported in works with surface modifications by sputtering, where an increase in the polarity of the surface by the formation of ordained groups can cause changes in the donors and receivers of electrons of the surface[1].

Table 2 Contact angle and surface energy for different coatings

Sample	Contact angle (°)	Surface energy (mJ/m^2)
0.1Q-PCL 120s Ag	66.38±0.02	43.95±0.01
0.1Q-PCL 240s Ag	21.05±0.02	68.36±0.01
0.2Q-PCL 120s Ag	47.41±0.01	55.25±0.01
0.2Q-PCL 240s Ag	29.82±0.01	64.56±0.01
0.3Q-PCL 120s Ag	30.52±0.05	64.23±0.02
0.3Q-PCL 240s Ag	18.45±0.28	69.32±0.10

The contact angle values were lower than 90° for all samples which indicate that they are hydrophilic. Wettability was strongly influenced by variations in the mixture of Q/PCL which was mentioned before. Other researchers have reported that it is not clear yet, which is the ideal contact angle to obtain the best results in the biological or clinical tests of biocompatibility [22]. However, hydrophilic surfaces in combination with the appropriate roughness conditions have shown increased bone cell growth [8, 23]. It is expected that for surfaces with greater roughness, the contact angle will be higher [8]. This was verified with the 0.1Q-PCL 120 Ag sample, which presented a higher Rq value and a contact angle of 66.38° is the highest value obtained in the whole group of characterized samples.

Surface energy is one of the most important characteristics parameters in cell adhesion. It is related to adhesion strength and has been reported as one of the most determinant factors in the definition of biocompatibility of biomaterials, rather than roughness [8, 24]. For this research, surface energy calculations were performed with the surface energy tool for a liquid, using DROPimage standard software from Ramé-Hart Instruments. The energy was calculated from Equation (1) which is the surface state equation and describes the correlation between the contact angle θ, the surface tension of the liquid γ_l, in this case, water and the surface energy of the solid, which in this case the coating [25].

$$\cos\theta + 1 = 2\sqrt{\frac{\gamma_s}{\gamma_l}}e^{-\beta(\gamma_l-\gamma_s)^2} \quad (1)$$

Where ß Is an experimentally determined constant:

$$\beta = 0.0001247(\frac{mN}{m})^{-2}$$

The software used an iteration process to solve the surface energy of the solid γ_s. For the different samples, a surface energy greater than 60 mJ/m2 was obtained except for the sample 0.1Q-PCL 120s Ag and 0.2Q-PCL 120s Ag. Previous works have concluded that cell adhesion and proliferation are mainly determined by the surface energy, which is influenced by the roughness [1, 7]. Surface energy values have been reported for polished Ti6Al4V samples of approximately 50 mJ/m^2, using calculation models with approximations obtained through the use of two liquids in contact angle measurements, one polar and one non-polar [1]. These values are very close to those reported in this work. These are related to an adequate wettability of the surface that allows the prediction of an increase in the interaction between the surface of the implant and the bone tissue. Another study has shown that cell propagation increases in substrates with higher surface energy, both in the presence and absence of protein adsorption [7]. Likewise, the work made by Ponsonnet et al. shows that for fibroblast cells the exchange value of surface energy between poor to good cell propagation is about 57mJ/m^2 [8].

4. Conclusions

Polymeric coatings with porous agglomerates on a substrate of Ti6Al4V were obtained using the dip-coating technique with components known to be antibacterial, such as chitosan and silver. It was possible to obtain a substrate composed of silver particles, deposited by sputtering, which remained during the treatment of dip-coating with the different solutions of Q-PCL used for this study. A higher concentration of chitosan incorporated into the solution with polycaprolactone was proportional to a decrease in the size of the agglomerates in the coating and directly proportional to the increase in wettability. The differences in the size of these agglomerates could be critical in the cell adhesion, proliferation, and differentiation processes. The presence of Q and PCL in the coatings could be corroborated by Raman confocal spectroscopy and with EFM the conductive properties of the coatings obtained favored by the presence of silver particles were observed. Critical synergies in the electrical properties, wettability, and morphology, are determinant in the definition of bioactivity of the coatings proposed in this research.

5. Acknowledgments

The authors acknowledge the funding of Sistema General de Regalías de Colombia (SGR) macroproyecto de salud BPIN code: 2012000100172.

References

[1] Y. Yan, E. Chibowski, and A. Szcześ, "Surface properties of Ti-6Al-4V alloy part I: Surface roughness and apparent surface free energy," *Mater. Sci. Eng. C.*, vol. 70, no. 1, pp. 207–215, Jan. 2017.

[2] Matykina and *et al.*, "Characterization of Spark-Anodized Titanium for Biomedical Applications," *Journal of The Electrochemical Society*, vol. 154, no. 6, pp. C279–C285, 2007.
[3] F. C. García, D. Y. Peña, and H. A. Estupiñán, "Comportamiento morfológico y electroquímico de un recubrimiento Dip Coating policaprolactona-quitosano-colágeno sobre Ti6Al4V," vol. 38, pp. 54–75, Apr. 2017.
[4] A. R. Sarasam, "Chitosan-polycaprolactone mixtures as biomaterials -influence of surface morphology on cellular activity," Ph.D. dissertation, Faculty of the Graduate College, Oklahoma State University, Oklahoma, EE. UU, 2006.
[5] S. W. Pok, K. N. Wallace, and S. V. Madihally, "In vitro characterization of polycaprolactone matrices generated in aqueous media," *Acta Biomater.*, vol. 6, no. 3, pp. 1061–1068, Mar. 2010.
[6] D. Campoccia, L. Montanaro, and C. R. Arciola, "A review of the biomaterials technologies for infection-resistant surfaces." *Biomaterials*, vol. 34, no. 34, pp. 8533–8554, 2013.
[7] G. Zhao, Z. Schwartz, M. Wieland, F. Rupp, J. Geis-Gerstorfer, D. L. Cochran, and B. D. Boyan, "High surface energy enhances cell response to titanium substrate microstructure." *Journal of biomedical materials research. Part A*, vol. 74, no. 1, pp. 49–58, 2005.
[8] L. Ponsonnet, K. Reybier, N. Jaffrezic-Renault, V. Comte, C. Lagneau, M. Lissac, and C. Martelet, "Relationship between surface properties (roughness, wettability) of titanium and titanium alloys and cell behaviour," vol. 23, pp. 551–560, Jun. 2003.
[9] L. Gómez, A. Quintero, D. Peña, and H. Estupiñan, "Obtención, caracterización y evaluación in vitro de recubrimientos de policaprolactona-quitosano sobre la aleación Ti6Al4V tratada químicamente," *Revista de Metalurgia*, vol. 50, no. 3, 2014.
[10] K. Wang, C. Zhou, Y. Hong, and X. Zhang, "A review of protein adsorption on bioceramics," *Interface focus*, vol. 2, pp. 259–77, Jun. 2012.
[11] M. P. Fiorucci, A. J. López, and A. Ramil, "Surface modification of ti6al4v by nanosecond laser ablation for biomedical applications," *Journal of Physics: Conference Series*, vol. 605, no. 1, p. 012022, 2015.
[12] F. Meng, Y. Liu, J. Chu, W. Wang, and T. Qi, "Structural control of Na_2Tio_3 in pre-treating natural rutile ore by alkali roasting for Tio_2 production," *Can. J. Chem. Eng.*, vol. 92, no. 8, pp. 1346–1352, Aug. 2014.
[13] L. G. R. y Andrés Quintero Jaime y Darío Peña Ballesteros y Hugo Estupiñan Durán, "Obtención, caracterización y evaluación in vitro de recubrimientos de policaprolactona-quitosano sobre la aleación Ti6Al4V tratada químicamente," *Revista de Metalurgia*, vol. 50, no. 3, 2014.
[14] A.L.Yerokhin, X.Nie, A.Leyland, and A.Matthews, "Characterisation of oxide films produced by plasma electrolytic oxidation of a Ti–6Al–4V alloy," *Surface and Coatings Technology*, vol. 130, no. 2-3, pp. 195–206, Aug. 2000.
[15] R. Briceño, S. Camero, G. Gonzáles, and A. Rosales, "Estudio de la susceptibilidad a la corrosión en presencia de fluidos corporales simulados de una aleación Ti6Al4V recubierta con hidroxiapatita," *Acta Microsc.*, vol. 21, no. 3, pp. 160–176, 2012.
[16] C. E. Bamberger and G. M. Begun, "Sodium Titanates: Stoichiometry and raman Spectra," *Journal of the American Ceramic Society*, vol. 70, no. 3, pp. C–48–C–51, Mar. 1987.
[17] J. Arnoux, G. Sutter, G. List, P. Bourson, and H. Chaynes, "Raman characterization of Ti–6Al–4V oxides and thermal history after kinetic friction," *Phase Transitions*, vol. 87, no. 6, Feb. 2014.
[18] M. Gaintantzopoulou, S. Zinelis, N. Silikas, and G. Eliades, "Micro-Raman spectroscopic analysis of TiO2 phases on the root surfaces of commercial dental implants," *Dent. Mater.*, vol. 30, no. 8, pp. 861–867, Aug. 2014.
[19] I. Martina, R. Wiesinger, D. Jembrih, and M. Schreiner, "Micro-Raman characterization of silver corrosion products: Instrumental set-up and reference database," vol. 9, pp. 1–6, Jan. 2012.
[20] P. Girard, "Electrostatic force microscopy: principles and some applications to semiconductors," *Nanotechnology*, vol. 12, no. Apr., p. 485.
[21] H. A. Estupiñan, C. Vázquez, D. Y. Peña, and L. F. Ardila, "Degradación de ácido poliláctico/hidroxiapatita y ácido poliglicólico en fluido corporal simulado," *Rev. UIS Ing.*, vol. 10, no. 2, pp. 145–150, Dec. 2011.
[22] G. Strnad, N. Chirila, C. Petrovan, and O. Russu, "Contact Angle Measurement on Medical Implant Titanium Based Biomaterials," *Procedia Technol.*, vol. 22, pp. 946–953, 2016.
[23] R. A.Gittens and *et al.*, "A review on the wettability of dental implant surfaces II: Biological and clinical aspects," *Acta Biomaterialia*, vol. 10, no. 7, pp. 2907–2918, Jul. 2014.
[24] N. J. Hallab, K. J. Bundy, K. O'Connor, R. L. Moses, and J. J. Jacobs, "Evaluation of Metallic and Polymeric Biomaterial Surface Energy and Surface Roughness Characteristics for Directed Cell Adhesion," *Tissue Eng.*, vol. 7, no. 1, pp. 55–71, Feb. 2001.
[25] D. Y. Kwok and A. W. Neumann, "Contact angle measurement and contact angle interpretation," *Adv. Colloid Interface Sci*, vol. 81, no. 3, pp. 167–249, Sep. 1999.